

Journal of the Brazilian Society of Mechanical Sciences and Engineering
Numerical study to investigate the effect of inlet velocity on thermal-fluid phenomena in
the supercritical carbon dioxide cooled pebble bed reactor
--Manuscript Draft--

Manuscript Number:	BMSE-D-15-01072
Full Title:	Numerical study to investigate the effect of inlet velocity on thermal-fluid phenomena in the supercritical carbon dioxide cooled pebble bed reactor
Article Type:	Technical Paper
Abstract:	<p>This paper presents a numerical investigation of thermal-fluid phenomena in a supercritical carbon dioxide cooled pebble bed reactor (SCPBR) core under steady state using computational fluid dynamic (CFD). In this study, a three-dimensional model with the capability to simulate fluid flow and heat transfer in the SCPBR core has been developed. The developed model was implemented on a personal computer using ANSYS Fluent 14.5. Several important fluid flow and heat transfer parameters have been examined; including the pressure drop over the reactor core, the heat transfer coefficient, the temperature distribution, the coolant density and the coolant velocity. Results obtained from the simulation show that with increasing the inlet velocity, the pressure drop, the coolant density and the heat transfer coefficient increases. However, the coolant temperature and the temperature difference between pebble and coolant decrease with increasing the inlet velocity. The conclusion of the analysis is that the supercritical carbon dioxide (S-CO₂) would be a suitable coolant for using in pebble bed reactor due to its heat transfer characteristic and large mass density, which could lead to obtain lower pressure drop and higher power density.</p>

[Click here to view linked References](#)1
2
3
4
5

Numerical study to investigate the effect of inlet velocity on thermal-fluid phenomena in the supercritical carbon dioxide cooled pebble bed reactor

6
7
8
9
10**Masoumeh Sadat Latifi^a, Saeed Setayeshi^a**11
12
13^a Dept. of Energy engineering and physics, Amirkabir University of Technology, Tehran, Iran.14
15
16
17
18
19
20

Abstract

21
22
23

This paper presents a numerical investigation of thermal-fluid phenomena in a supercritical carbon dioxide cooled pebble bed reactor (SCPBR) core under steady state condition using computational fluid dynamic (CFD). In this study, a three-dimensional model with the capability to simulate fluid flow and heat transfer in the SCPBR core has been developed. The developed model was implemented on a personal computer using ANSYS Fluent 14.5. Several important fluid flow and heat transfer parameters have been examined; including the pressure drop over the reactor core, the heat transfer coefficient, the temperature distribution, the coolant density and the coolant velocity. Results obtained from the simulation show that with increasing the inlet velocity, the pressure drop, the coolant density and the heat transfer coefficient increases. However, the coolant temperature and the temperature difference between pebble and coolant decrease with increasing the inlet velocity. The conclusion of the analysis is that the supercritical carbon dioxide ($S\text{-CO}_2$) would be a suitable coolant for using in pebble bed reactor due to its heat transfer characteristic and large mass density, which could lead to obtain lower pressure drop and higher power density.

46
47
48
49
50
51*Keywords:* CFD, heat transfer, $S\text{-CO}_2$, SCPBR, inlet velocity52
53
54
55
56
57
58
59
60
61
62
63
64
65

Nomenclature

d	diameter of the fuel sphere (pebble)
d_{peb}	diameter of pebble
e	emissivity of pebble
G_K	generation of turbulence kinetic energy

1	
2	
3	
4	h_{sf} fluid–solid heat transfer coefficient
5	
6	
7	k turbulence kinetic energy
8	
9	
10	k_{eff} effective thermal conductivity
11	
12	
13	k_f fluid thermal conductivity
14	
15	k_{peb} thermal conductivity of pebble
16	
17	k_s solid thermal conductivity
18	
19	p pebble bed packing fraction
20	
21	P pressure
22	
23	u superficial mean exit velocity
24	
25	S_h heat source
26	
27	T Pebble temperature
28	
29	ΔT inlet-outlet temperature difference
30	
31	
32	v velocity
33	
34	
35	Greek letters
36	
37	ϵ bed porosity
38	
39	ϵ_e energy dissipation rate
40	
41	ϵ_b volumetric porosity
42	
43	μ dynamic viscosity
44	
45	μ_t turbulent viscosity
46	
47	ρ fluid density
48	
49	ρ_{fuel} power density of each fuel sphere
50	
51	σ Stefan-Boltzmann constant
52	
53	
54	
55	
56	
57	
58	
59	
60	
61	
62	
63	
64	
65	

1. Introduction

The technology of the high temperature gas-cooled reactor (HTGR) is receiving increasing interest around the world. Two main types of HTGRs are pebble bed reactors (PBR) and prismatic block reactors (PMR). The pebble bed reactor (PBR) design consists of spherical fuel elements called pebbles. The 6 cm diameter pebble is made of pyrolytic graphite containing thousands microscopic fuel Tristructural-Isotropic (TRISO) particles. Each fuel pebble contain 9 grams of uranium to provide a low power density in the core. The low power density and the large graphite core provide inherent safety features in the HTGR design [1]. The traditional pebble bed reactor (PBR) is a graphite-moderated, gas-cooled reactor. The preferred coolant is helium, though carbon dioxide and nitrogen have been suggested too.

A review of the literature indicates a lot of numerous numerical studies on the fluid flow and heat transfer by simulating the pebble bed reactor core as a porous media. Several simulation works [2-6] have demonstrated that a model with the porous approach could predict the distributions of flow velocity, temperature, pressure, etc reasonably. Latifi et al [7] developed a two-dimensional CFD model to investigate the effect of porosity on the thermal-fluid phenomena in pebble bed modular reactor core (PBMR) by considering the core as a porous media. Y.M. Ferng et al [8] presented a numerical study of thermal-fluid phenomena in a pebble bed helium-cooled reactor (HTR-10) core under steady state and accident conditions using computational fluid dynamic (CFD) to investigate the thermal-hydraulic characteristics within the HTR-10 core. Oukil et al [9] presented a mathematical model based on porous media theory to evaluate the convective heat transfer for different ratios of internal and external radius and for different Biot numbers, for both air and helium.

S-CO₂ cooled pebble bed reactor (SCPBR) is selected for the present simulations. The supercritical CO₂ (S-CO₂) has attracted great interest as coolants due to they can use in both direct and indirect cycles. Application of S-CO₂ at a medium temperature (923K) gives a thermodynamic productivity near to that of helium at high temperature. The disadvantage of S-CO₂ is the high pressure (25 MPa), potentially resulting in a large void effect [10].

In this study, in order to minimize the overall size of nuclear plant, the direct S-CO₂ Brayton cycle has been chosen. To study the thermal hydraulic characteristics of S-CO₂ cooled pebble bed reactor (SCPBR), CFD methods have been adopted to simulate flow and heat transfer in the SCPBR core.

In this paper, a three-dimensional CFD model is developed to investigate the thermal-hydraulic characteristics within the core under steady-state conditions. The model examines the effect of inlet velocity on the thermal-hydraulic phenomena in the SCPBR core. In this model, several important fluid flow and heat transfer parameters are examined, including the pressure drop over the reactor core, the heat transfer coefficient, etc.

In order to investigate the effect of the inlet velocity on the thermal-hydraulic behavior of the core under steady state condition, various values of inlet velocity were selected namely 0.75m/s, 1m/s, 1.5m/s and 2m/s.

2. Mathematical Model

The governing equations used to simulate the thermal-fluid characteristic of the SCPBR core under steady state condition include the continuity equation, the momentum equation, the energy equation and the k- ϵ two- equation turbulence model. In order to simulate the closely packed pebbles in the core, the porous medium is used. [11, 12]:

2.1. Governing equations

2.1.1. Continuity equation

$$\frac{\partial(\varepsilon\rho)}{\partial t} + \nabla \cdot (\varepsilon\rho\vec{v}) = 0 \quad (1)$$

2.1.2. Momentum equation

$$\frac{\partial(\varepsilon\rho\vec{v})}{\partial t} + \nabla \cdot (\varepsilon\rho\vec{v}\vec{v}) = -\varepsilon\nabla P + \nabla \cdot (\varepsilon\vec{\tau}) + \varepsilon\rho\vec{g} - \nabla P_{Porous} \quad (2)$$

where ∇P_{Porous} is the extra pressure drop due to the presence of fuel spheres inside the core, which demonstrated by modified Ergun correlation as follows [13-15].

$$\nabla P = -180 \frac{(1-\varepsilon)^2}{\varepsilon^3} \frac{\mu\vec{u}}{d^2} - 1.8 \frac{1-\varepsilon}{\varepsilon^3} \rho \frac{|\vec{u}| \vec{u}}{d} \quad (3)$$

2.1.3. Energy equation

Fluid phase

why didn't you consider
time-term for fluid
temperature eqn.?

$$[(\rho c_p)_f \varepsilon] (\nabla \cdot (u T_f)) = \nabla \cdot (K_{eff} \nabla T_f) + h_{sf} a_{sf} (T_s - T_f) \quad (4)$$

Solid phase

$$[(\rho c_p)_s (1-\varepsilon)] \left(\frac{\partial T_s}{\partial t} \right) = \nabla \cdot (K_{eff} \nabla T_s) - h_{sf} a_{sf} (T_s - T_f) + S_h \quad (5)$$

where k_{eff} is the effective thermal conductivity of the packed bed and described by [16]:

$$k_{eff} = \varepsilon k_f + (1-\varepsilon) k_s \quad (6)$$

where k_s is solid thermal conductivity which accounts for both conduction and radiation heat transfers between pebbles. This is demonstrated by modified Zehner – Schulnder correlation as follows

$$k_s = 4\sigma T^3 d_{peb} \left\{ \left[1 - p^{0.5} \right] (1-p) + \frac{p^{0.5}}{\frac{2}{e} - 1} \left(\frac{B_z + 1}{B_z} \right) \left[1 + \frac{1}{(\frac{2}{e} - 1) K_{peb}} \right]^{-1} \right\} \quad (7)$$

$$\text{where } B_z = 1.25 \left(\frac{p}{1-p} \right)^{10/9}$$

The last term in Eq. (5), S_h (W/m³) is the heat source generated by nuclear chain reactions.

2.2. $k-\varepsilon$ Turbulence equation

The standard $k-\varepsilon$ turbulence model is applied in the present simulation. The turbulence kinetic energy, k , and energy dissipation rate, ε_e are obtained by using the following transport equations [17, 18].

$$\frac{\partial(\rho k)}{\partial t} + \nabla \cdot (\rho \bar{u} k) = \nabla \cdot \left((\mu + \frac{\mu_t}{\sigma_k}) \nabla k \right) + G_k - \rho \varepsilon_e \quad / \quad (8)$$

$$\frac{\partial(\rho \varepsilon_e)}{\partial t} + \nabla \cdot (\rho \bar{u} \varepsilon_e) = \nabla \cdot \left((\mu + \frac{\mu_t}{\sigma_\varepsilon}) \nabla \varepsilon_e \right) + \frac{\varepsilon_e}{k} (C_{\varepsilon 1} G_K - C_{\varepsilon 2} \rho \varepsilon_e) \quad / \quad (9)$$

where μ_t , turbulent viscosity is modeled by

$$\mu_t = \rho C_\mu \frac{k^2}{\varepsilon_e} \quad / \quad (10)$$

and G_K represents the generation of turbulence kinetic energy, given by:

$$G_k = (\mu + \mu_t) \nabla \bar{v} \cdot [\nabla \bar{v} + (\nabla \bar{v})^T] \quad / \quad (11)$$

$C_\mu=0.09$, $C_{\varepsilon 1}=1.44$, $C_{\varepsilon 2}=1.92$, $\sigma_k=1$, $\sigma_\varepsilon=1.3$ are empirical constants for turbulent models.

2.3. Porosity

As previously mentioned, the core region can be assumed as a porous medium. In a randomly packed bed of spheres, the average porosity, away from the walls, varies from 0.36 to 0.43[15]. Close to the wall, porosity is not uniform [19]. In the SCPBR core, there is no tangential variation in the porosity. For this study, the variation in the radial direction was assumed to be exponential. The annular core is filled with the pebbles and is bounded in the radial direction by center reflector and side reflector. Therefore, the effect of the core walls on the radial porosity distribution can be explained using the following equations [20].

$$\varepsilon(r) = \varepsilon_b \left[1 + C \exp(-N \frac{r - R_i}{d_{peb}}) \right], R_i \leq r \leq \frac{R_o + R_i}{2} \quad / \quad (12)$$

$$\varepsilon(r) = \varepsilon_b \left[1 + C \exp(-N \frac{R_o - r}{d_{peb}}) \right], \frac{R_i + R_o}{2} \leq r \leq R_o \quad / \quad (13)$$

where, ε_b , the volumetric porosity is the fraction of the void volume over the total volume. Fig.1 shows that the porosity varies as a function of distance from the wall.

Fig1

1
2
3
4
5
6 *2.4. Boundary conditions*

7
8
9 A simple geometry of the SCPBR core is shown in Fig.2 in which the S-CO₂ (coolant) enters from the top of the
10 core at a temperature of 773 K and at a pressure of about 20 Mpa. The main parameters of the core are described in
11 Table 1. The gas moves downward between the hot fuel pebbles, after which it leaves the reactor core at the bottom
12 of the vessel. The no-slip condition is assumed at the walls. The power density of each fuel sphere would be 7.8
13 MW/m³. Constant temperature boundary condition at the pressure vessel outer wall is 564 K. Adiabatic boundary
14 condition can be assumed for top and bottom walls. The other boundary conditions for this simulation are shown in
15 Table 2.

16
17
18 For different values of the inlet velocity (0.75, 1, 1.5 and 2 m/s), flow and heat transfer are simulated in a three-
19 dimensional model.

20
21
22 **Fig2**

23
24
25
26 **Table1:** SCPBR parameters

27
28
29
30
31
32 **Table 2:** Boundary conditions for numerical simulation

33
34
35
36
37 **3. Numerical method**

38
39
40
41
42
43
44 The finite volume based commercial CFD code ANSYS Fluent 14.5 was used to simulate the thermal-hydraulic
45 phenomena of the HTGR core. The pressure-velocity coupling was handled by the SIMPLE [21, 22] algorithm. The
46 second order upwind discretization scheme was used for the energy, momentum, turbulent kinetic energy, and
47 turbulent dissipation rate, whereas the pressure field was discretized with the PRESTO! scheme [21]. The relaxation
48 factors were 0.3 for pressure, 0.6 for momentum, 0.3 for density, 0.6 for turbulent kinetic energy, 0.8 for turbulent
49 dissipation rate, and 0.7 for energy. The convergence criteria were set at 10⁻⁴ for velocity and 10⁻⁶ for energy
50 equation and 10⁻³ for continuity.

1
2
3
4
5

4. Mesh independence study

6
7
8
9
10
11
12
13
14
15

In order to investigate grid independency of the simulation, various meshes have been employed, namely 162438, 288410, 1021884 cells, respectively. From Fig.3 it is observed that the temperature distributions along the axial position of the core are almost the same for the three grids used. This means that the difference in the three grid systems used in the simulations makes only a small deviation to the numerical predictions. Thus, considering time and memory, grid size of 288410 was selected.

16
17
18
19
20
21
22
23
24
25
26
27
28
29
30
31
32
33
34
35
36
37
38
39
40
41
42
43
44
45
46
47
48
49
50
51
52
53
54
55
56
57
58
59
60
61
62
63
64
65

T is not a primary quantity and therefore
should not be used to assess mesh
independence (or ergodicity)!

Fig3

5. Results and discussion

Fig.4 shows the temperature distribution along the axial position of the core under the steady state condition for different four inlet velocities (0.75 m/s, 1 m/s, 1.5 m/s, 2 m/s). The coolant temperature increases due to absorbing heat from the fuel spheres as the coolant flows through the core and the maximum value of the temperature occurs in the vicinity of the outlet, as shown in Fig.4a. As can be seen from Fig.4 the solid temperature and the coolant temperature decreases with an increase in the inlet velocity. This is due the fact that an increase in the inlet velocity leads to increase in volumetric flow rate of the coolant, so for a given energy source, the inlet-outlet temperature difference decreases with increasing inlet velocity and then for a given inlet temperature (i.e. 773K), the outlet temperature increases with decreasing inlet velocity.

Fig4

Fig.5 shows the temperature distribution along the radial direction of the core for different four inlet velocities. As mentioned before, the coolant temperature decreases with an increase in the inlet velocity. However, as can be seen, the coolant temperature is constant along the radial direction of the core. There are a lot of parameters affects the radial distribution of the coolant temperature. One of them is the direction of the coolant flow. In this case, the direction of the coolant flow is downward and along the axial position of the core. Therefore, the specifics of coolant

flow along the radial direction remains constant such as velocity. Thus, the coolant temperature remains constant along the radial direction of the core.

Fig5

Fig6

↓ based on assumption
the S_b is constant!

But what about wall-fluid &
wall-solid heat transfer effects?

As mentioned before, the velocity remains constant along the radial direction of the core as shown in Fig.6. Fig.6 shows contour plots of coolant velocity in the radial direction for four different inlet velocity values under steady state condition; these curves are for a height of 2.25 m in the core. As shown in this figure, away from the wall, the fluid velocity is uniform, but near the wall, this is not the case because of variation in the porosity near the wall. From Fig.1, close to the wall the porosity increases to about twice the bulk porosity (ϵ_b), which causes a major decrease in fluid velocity. Since with increasing porosity, the diameter of the pores increases and so for a certain volumetric flow rate, the velocity decreases. From Fig. 6, it is evident that the lowest value of velocity occurs with lowest inlet velocity. Specifically, for an inlet velocity of 0.75 m/s, the fluid velocity takes its minimum value, $v = 0.049$ m/s.

As shown in Fig.7, the coolant density decreases from inlet ($z=4.5$ m) to outlet ($z=0$). This is due the fact that the coolant velocity increases downstream of the core due to the temperature increase, so for a given mass flow rate, the fluid density decreases from inlet to outlet. However, as shown in this figure, with increasing the value of inlet velocity, the fluid density increases. Since the fluid density depends on the coolant temperature indirectly and with increasing the fluid temperature, it decreases. Then, as mentioned before, with increasing inlet velocity, the coolant temperature decreases and so the coolant density increases. From Fig.7, it is evident that the highest value of coolant density occurs with lowest temperature (i.e. inlet temperature) that is equal for all of cases (i.e. 773 K). Thus, for all four inlet velocities, the fluid density takes its maximum value at the inlet ($z=4.5$ m), $\rho = 133.9$ kg/m³.

Fig7

Fig8

$$\rho = \rho(P, T)$$

Fig.8 shows the pressure drop along the axial position of the core at different inlet velocities (0.75 m/s, 1 m/s, 1.5 m/s, 2 m/s). As revealed from this figure, the pressure drop increases along the axial position of the core with increasing the inlet velocity. It should be noted that according to Ergun equation, the pressure drop depends on the fluid density and fluid velocity, so the pressure drop is proportional to the square of the flow rate. As seen before, the fluid density increases with increasing inlet velocity, then pressure drop increases with increasing inlet velocity. Specifically, for inlet velocity of 2 m/s, the pressure drop takes its maximum value, $p = 345657 \text{ Pa}$.

Fig9

Fig.9 shows a comparison between the numerical simulations for the local heat transfer coefficient and the theoretical results for inlet velocity of 0.75 m/s. The heat transfer coefficient is estimated from the thermal solution to the CFD model by using the following definition for the heat transfer coefficient:

$$q'' = h(T_s - T_f) \quad (14)$$

where q'' is the heat flux (W/m^2), T_s is the average surface temperature of a particular pebble (K) and T_f is the temperature of the coolant in the vicinity of the pebble (K).

The local heat transfer coefficients between pebbles and coolant also is estimated using the Heil correlation [23]:

$$h = 0.68 \rho v C_p Re^{-0.2} Pr^{-0.66} \quad (15)$$

$$Re = \frac{\rho v d}{(1-\varepsilon)\mu} \quad (16)$$

The KTA rules*correlation for heat transfer within a PBR is defined by the following equations (for Nusselt number and hear transfer coefficients) [24].

$$h = \frac{Nu \lambda}{d} \quad (17)$$

$$Nu = 1.27 \frac{Pr^{1/3}}{x^{1/18}} Re^{0.26} + 0.033 \frac{Pr^{1/2}}{x^{1/07}} Re^{0.86} \quad (18)$$

As shown in Fig.9 the local heat transfer is a bit smaller than the KTA calculated, due to slightly out of utilization range for Reynolds number, and it is a bit bigger than the Heil calculated. From this figure, it is evident that there is a better agreement between the CFD results and the calculations of Heil correlation. This due the fact that in the current study, the Reynolds number criteria (criteria of KTA) can not be met exactly.

1
2
3
4 Fig.10 illustrates the distribution of the local heat transfer coefficient along the axial direction of the core for
5 different values of the inlet velocity. As shown in this figure, local heat transfer coefficient increases with the
6 increase in the inlet velocity. In addition, it is clear that the local heat transfer coefficient increases along the core
7 with its highest value close to the outlet of the core. This is due the fact with increasing the fluid velocity, the
8 Reynolds number increases, so the local heat transfer coefficient, which is a function of Reynolds number increases.
9
10 For inlet velocity of 2 m/s, the local heat transfer coefficient takes its maximum value, $h= 5618.7$ (W/m²K).
11
12
13
14
15

16 Fig10
17
18

19 Fig11
20
21
22
23
24
25
26
27
28
29
30
31
32
33
34
35 According to Eq.14, it is obvious that with increasing the local heat transfer coefficient, the temperature difference
36 between pebble and coolant decreases as shown in Fig.11. From Fig. 11, it is evident that the highest value of ($T_s - T_f$)
37 occurs with lowest inlet velocity (i.e. 0.75m/s) and the lowest value of ($T_s - T_f$) occurs with the highest inlet
38 velocity (i.e. 2m/s).
39
40
41
42
43
44
45
46
47
48
49
50
51
52
53
54
55
56
57
58
59
60
61
62
63
64
65

6. Conclusions

A computational study has been performed to study the effects of inlet velocity on the thermal- fluid phenomena in the SCPBR core. The following trends have been identified:

- For constant heat flux, the coolant temperature decreases with increasing inlet velocity. The inlet-outlet temperature difference decreases with increasing inlet velocity and then for a given inlet temperature (i.e. 773k), the outlet temperature increases with decreasing inlet velocity and so the maximum value of the coolant temperature occurs with the lowest inlet velocity (i.e. 0.75m/s)
- The coolant density decreases from inlet ($z=4.5$ m) to outlet ($z=0$) due to increasing coolant velocity. However, with increasing the value of inlet velocity, the fluid density increases. This is due to the fact that the coolant density indirectly depends on the coolant temperature and with increasing the fluid temperature, it decreases. Then, as result shown in this paper, with increasing inlet velocity, the coolant temperature decreases and so the coolant density increases.

- 1
2
3
4 • According to Ergun equation, it is evident that the pressure drop depends on the fluid density and fluid
5 velocity, so the pressure drop is proportional to the square of the flow rate. Thus, the pressure drop
6 increases along the axial position of the core with increasing the inlet velocity.
7
8
9
10 • The local heat transfer coefficient increases with the increase in the inlet velocity. In addition, it is clear
11 that the local heat transfer coefficient increases along the core with its highest value close to the outlet of
12 the core. It is obvious that with increasing the local heat transfer coefficient, the temperature difference
13 between pebble and coolant decreases.
14
15

16
17
18
19 The conclusion of the analysis is that the supercritical carbon dioxide (S-CO₂) would be a suitable coolant for using
20 in pebble bed reactor due to its heat transfer characteristic and large mass density, which could lead to obtain lower
21 pressure drop and higher power density.
22
23
24
25
26
27
28 **References**
29
30
31
32 [1] Lohnert, G., 1990. Technical design features and essential safety-related properties of the HTR-module. Nuclear
33 Engineering and Design 121, 259–275
34
35 [2] W. Guo, A. Ying, M.J. Ni, M.A. Abdou, Influence of 2D and 3D convection-diffusion flow on tritium
36 permeation in helium cooled solid breeder blanket units, Fusion Eng. Des 81 (2006) 1465-1470.
37
38 [3] W.J. Van Rooyen, D.L.W. Krueger, E.H. Mathews, M. Kleingeld, Simulation and optimisation of gas storage
39 tanks filled with heat sink, Nucl. Eng. Des 236 (2006) 156-163.
40
41 [4] J. Van Der Merwe, J.P. Van Ravenswaay, Flownex Version 6.4 User Manual. MTech Industrial, Potchefstroom,
42 South Africa, 2003.
43
44 [5] S. Becker, E. Laurien, Three-dimensional numerical simulation of flow and heat transport in high-temperature
45 nuclear reactors, Nucl. Eng. Des 222 (2003) 189-201.
46
47 [6] P.G. Rousseau, C.G. du Toit, W.A. Landman, Validation of a transient thermal-fluid systems CFD model for a
48 packed bed high temperature gas-cooled nuclear reactor, Nucl. Eng. Des 236 (2006) 555-564.
49
50 [7] M.S. Latifi, S. Setayeshi, Effects of Porosity on Thermal-Fluid Phenomena in PBMR Core, Journal of Thermal
51 Engineering, 2016-2-2-April.
52
53 [8] Y.M. Ferng, C.T. Chen, CFD investigating thermal-hydraulic characteristics and hydrogen generation from
54 graphite-water reaction after SG tube rupture in HTR-10 reactor, Applied Thermal Engineering 31(2011)2430-2438.
55
56 [9] Kh. Oukil, K. Sidi-Ali, A. Alem, T. Hassani, Y. Amri, Porous media applied to pebble bed modular reactor
57 thermal-hydraulics, Journal of Science Research N 6, p. 19-23

↳ ? Year ?

- 1
2
3
4 [10] W.F.G. Van Rooijen, Improving fuel cycle design and safety characteristics of a gas cooled fast reactor, IOS
5 Press November 1, 2006
6
7 [11] F. Reitsma, G. Strydom, J.B.M. de Haas, K. Ivanov, B. Tyobeka, R. Mphahlele, T.J. Downar, V. Seker, H.D.
8 Gougar, D.F. Da Cruz, U.E. Sikik, The PBMR steady-state and coupled kinetics core thermal-hydraulics benchmark
9 test problems, Nuclear Engineering and Design 236 (2006) 657–668
10
11 [12] Chang Oh, Eung Kim, Richard Schultz, Mike Patterson, and David Petti, Thermal Hydraulics of the Very High
12 Temperature Gas Cooled Reactor, The 13th International Topical Meeting on Nuclear Reactor Thermal Hydraulics
13 (NURETH-13) Kanazawa, Japan. September 27-October 2, 2009.
14
15 [13] Ergun, S., Fluid Flow Through Packed Columns. Chemical Process Engineering, 1952. 48(2): p. 89-94.
16
17 [14] Macdonald, I.F., et al., Flow through Porous Media-the Ergun Equation Revisited. Ind. Eng. Chem. Fundam.,
18 1979. 18(3): p. 199-208.
19
20 [15] Kaviany, M., Principles of heat transfer in porous media, Springer.
21
22 [16] Hsu, C.-T., Heat Conduction in Porous Media in Handbook of Porous media, K. Vafai, Editor. 2000, Marcel
23 Dekker, Inc.: New York, NY.
24
25 [17] B.E. Launder, D.B. Spalding, The numerical computational of turbulent flows, Comp. Method Appl. Mech.
26 Eng. 3 (1973) 269.
27
28 [18] Ismail B. Celik, Introductory Turbulence Modeling, West Virginia University Mechanical & Aerospace
29 Engineering Dept. December, 1999.
30
31
32 [19] Benenati, R.F. and C.B. Browsilow, Void Fraction Distribution in Beds of Spheres. A. I. Ch. E., 1962. 8(3): p.
33 359-361.
34
35 [20] Vortmeyer, D., Schuster, J. Evaluation of steady flow profiles in rectangular and circular packed beds by a
36 variational method. Chemical Engineering Science 38, 1691–1699, 1983.
37
38 [21] S. V. Pantankar, Numerical heat transfer and fluid flow, first ed. Hemisphere Publishing, Washington,
39 DC, 1980.
40
41 [22] Joel H. Ferziger, Milovan Peric', Computational methods for fluid dynamics, third ed., Springer, 2002.
42
43 [23] Heil, J, et al. Zusammenstellung von Gleichung fuer den Druckverlust und den Wärmeübergang fuer
44 Stroemungen in Kugelschuttungen und prismatischen kanalen” , IRE/I-20 ((1969). Heil, 1969)
45
46 [24] Nuclear Safety Standards Commission (KTA), 1983. KTA 3102.2 Reactor Core Design of High-Temperature
47 Gas-Cooled Reactors. Part 2: Heat Transfer in Spherical Fuel Elements.
48
49
50
51
52
53
54
55
56
57
58
59
60
61
62
63
64
65

void follow d
styles!

1
2
3
4 **Caption figures**
5
6
7
8
9
10
11
12
13
14
15
16
17
18
19
20
21
22
23
24
25
26
27
28
29
30
31
32
33
34
35
36
37
38
39
40
41
42
43
44
45
46
47
48
49
50
51
52
53
54
55
56
57
58
59
60
61
62
63
64
65

Fig.1. The porosity variation as a function of distance from wall

Fig.2. A simplified geometry used in the computations

Fig.3. Mesh Independence Study

Fig.4. The inlet velocity effect on average temperature across the height of the core: a) the fluid temperature, b) the solid temperature

Fig.5. The inlet velocity effect on the fluid temperature across the radial direction of the core

Fig.6. Contour plot of the fluid velocity along the radial direction of the core in different inlet velocities: a) $v = 0.75$ m/s 0.36, b) $v = 1$ m/s, c) $v = 1.5$ m/s, d) $v = 2$ m/s

Fig.7. The inlet velocity effect on the fluid density across the height of the core

Fig.8. The inlet velocity effect on the pressure drop over the reactor core

Fig.9. Comparison of the heat transfer coefficient for velocity of 0.75 m/s

Fig.10. The inlet velocity effect on the heat transfer coefficient

Fig.11. The inlet velocity effect on the temperature difference between pebble and coolant

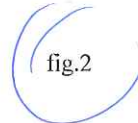


Table1

Constant core parameters	
Core thermal power (MW)	200
Power density of fuel sphere (MW/m ³)	7.8
Core inlet temperature (K)	773
System operating pressure (MPa)	20
Pressure vessel	Steel
Coolant flow direction	Down wards
Core outer diameter (m)	3.7
Core inner diameter (m)	2m
Core height (m)	4.5m
Porosity of the bed	0.4
Spherical fuel element diameter (cm)	6

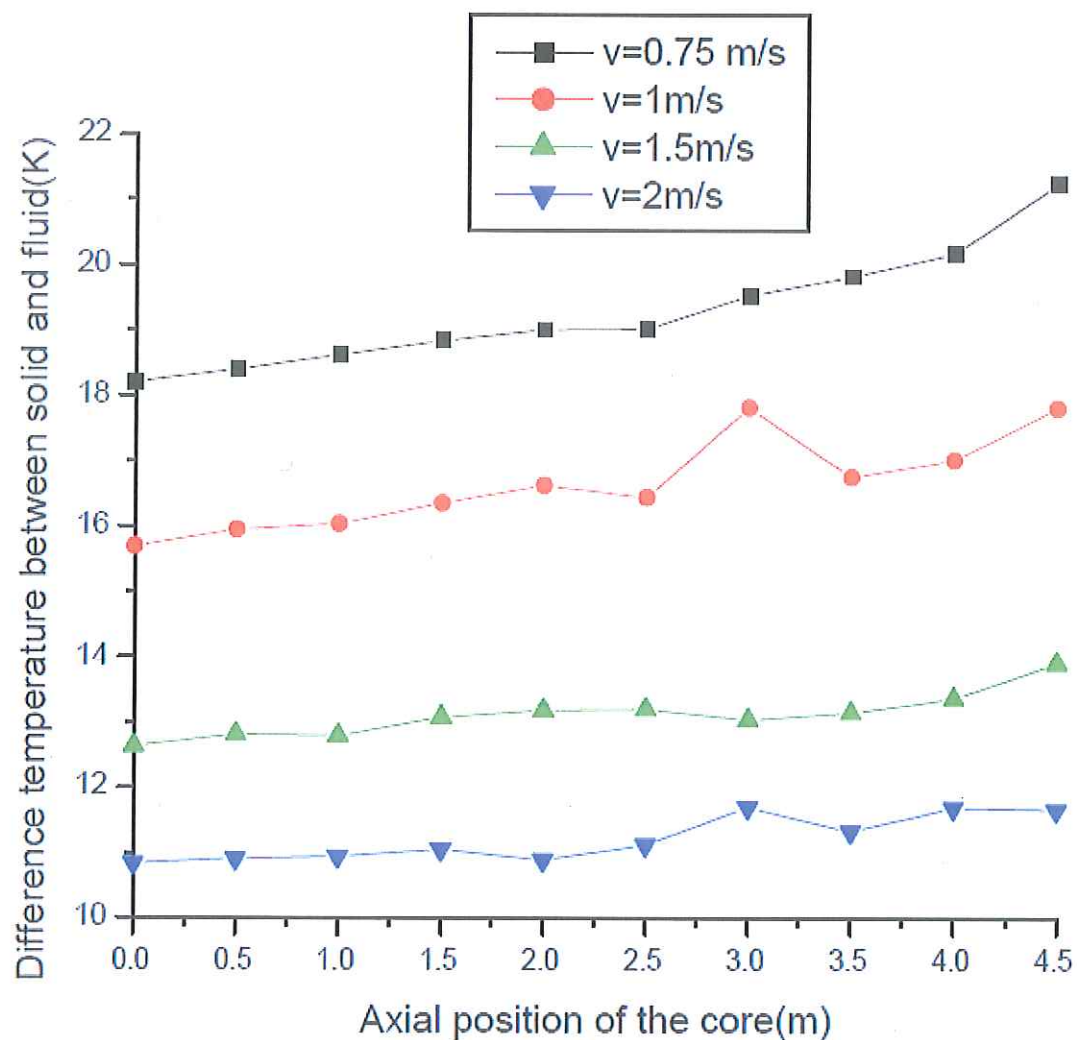


Fig.11

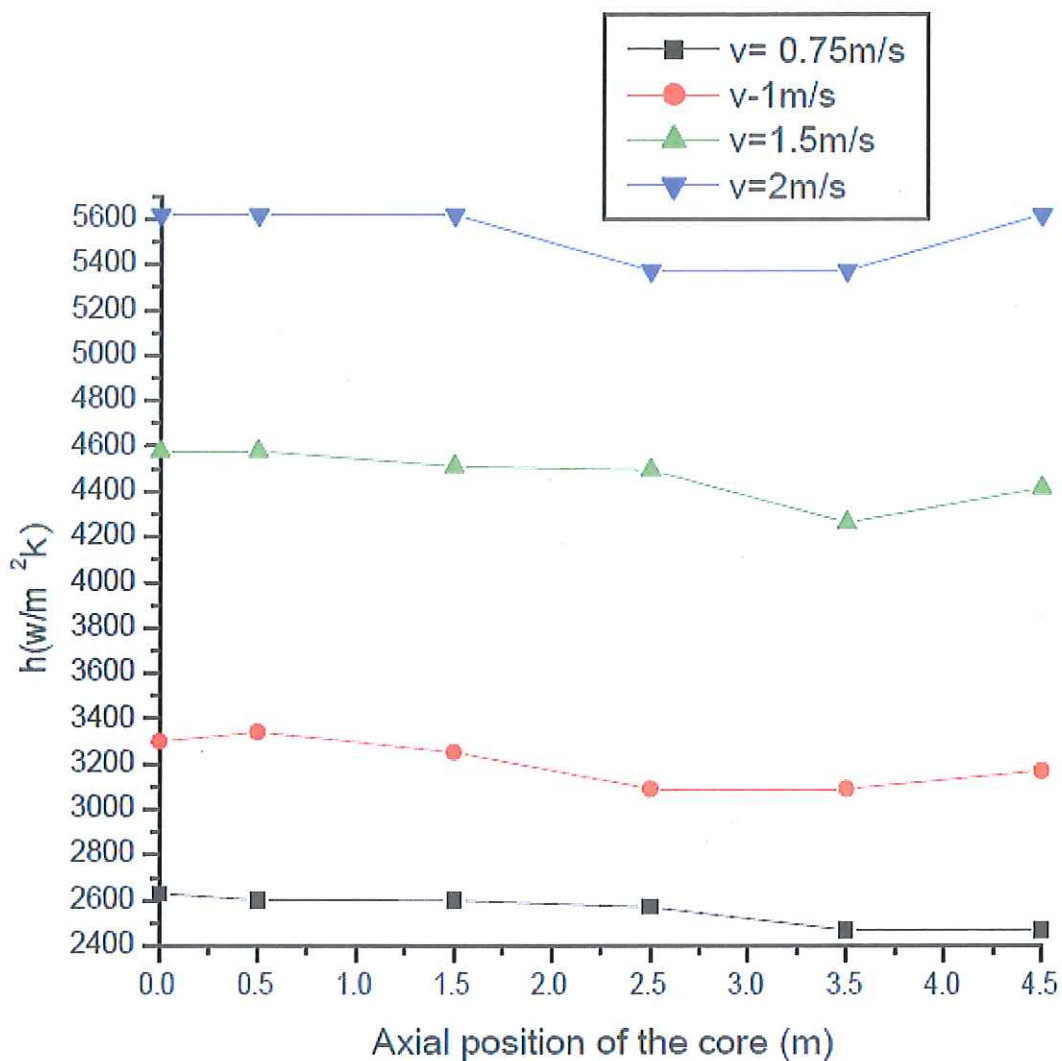


Fig 10

Which condition?

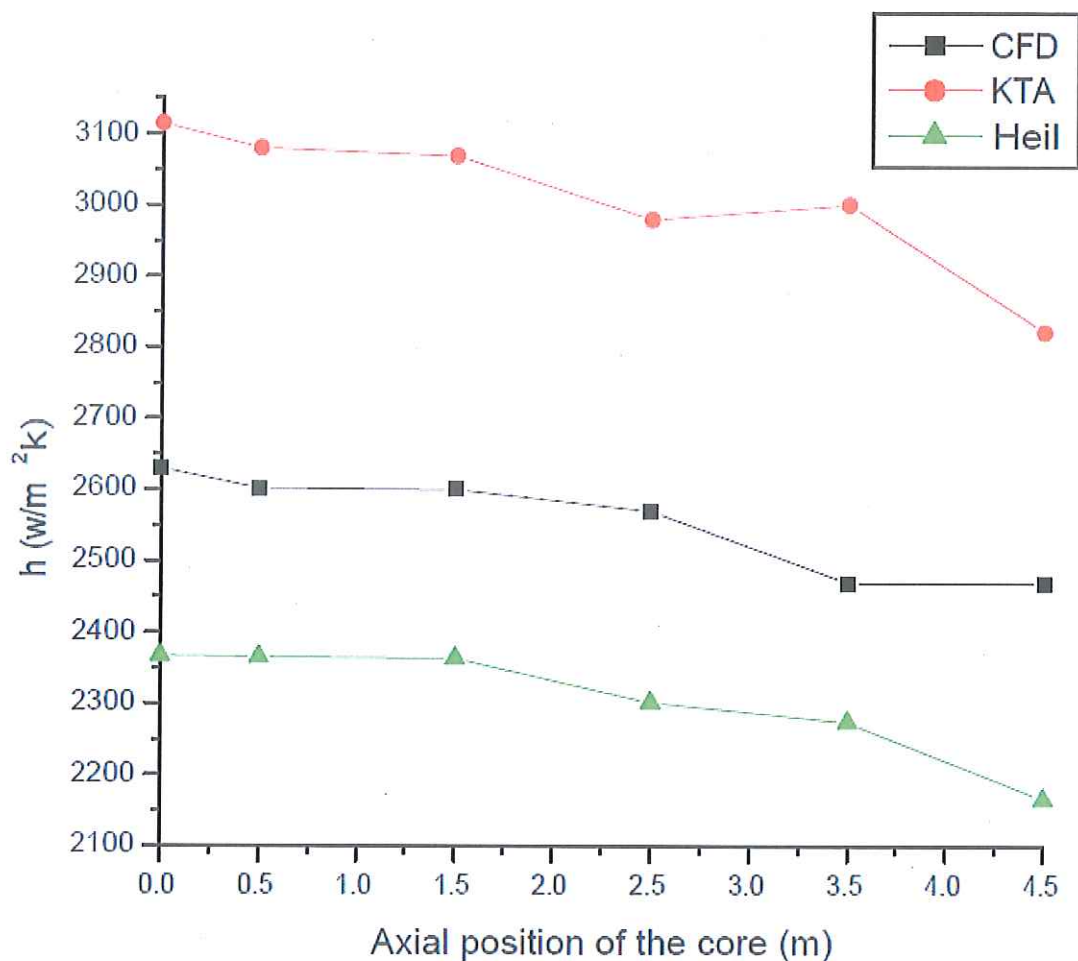


Fig.9

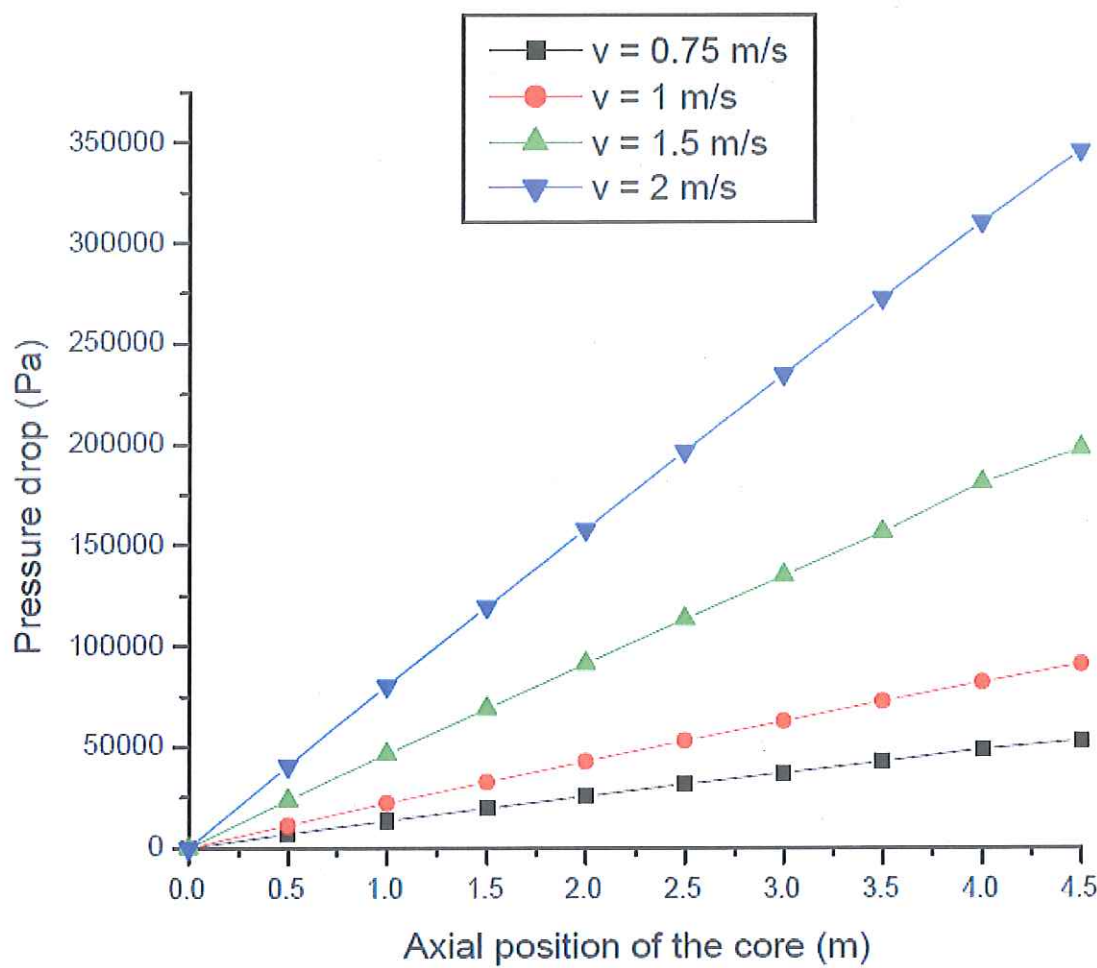


Fig 8

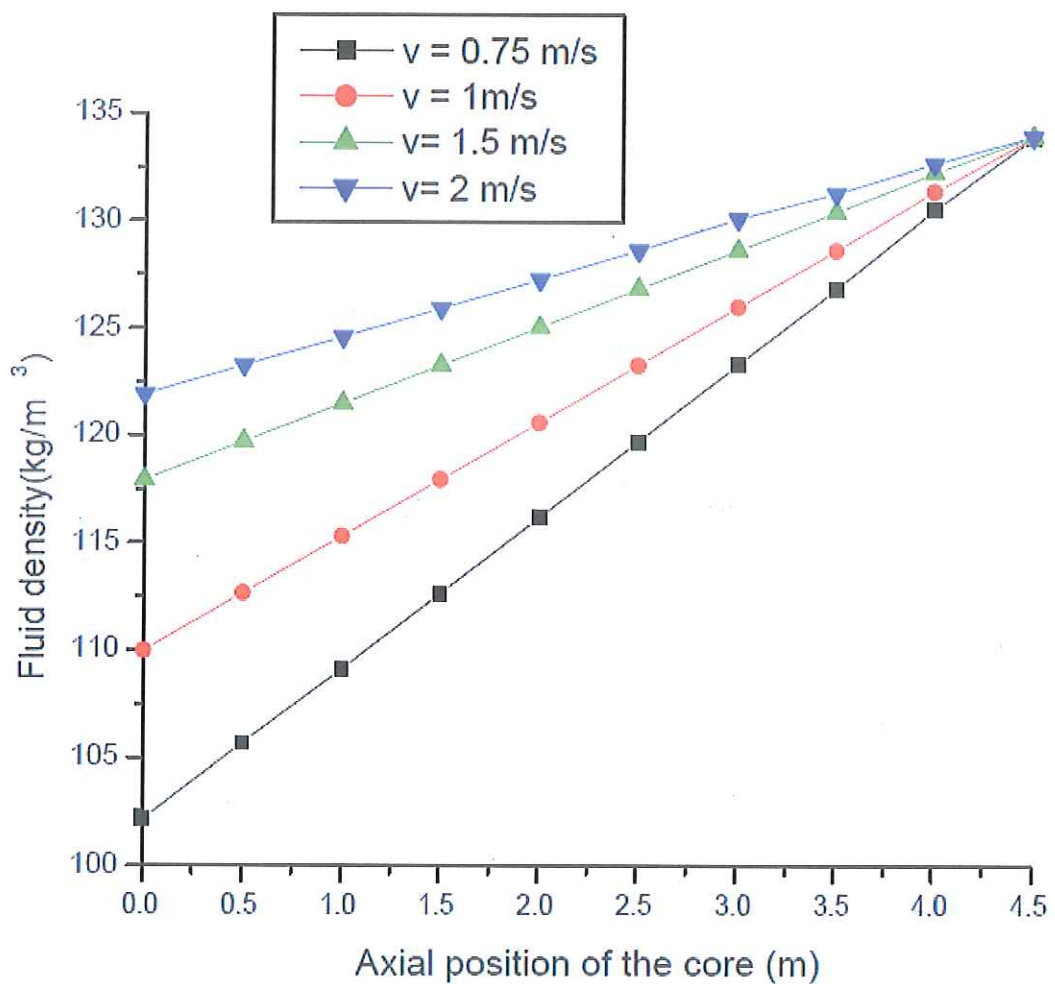
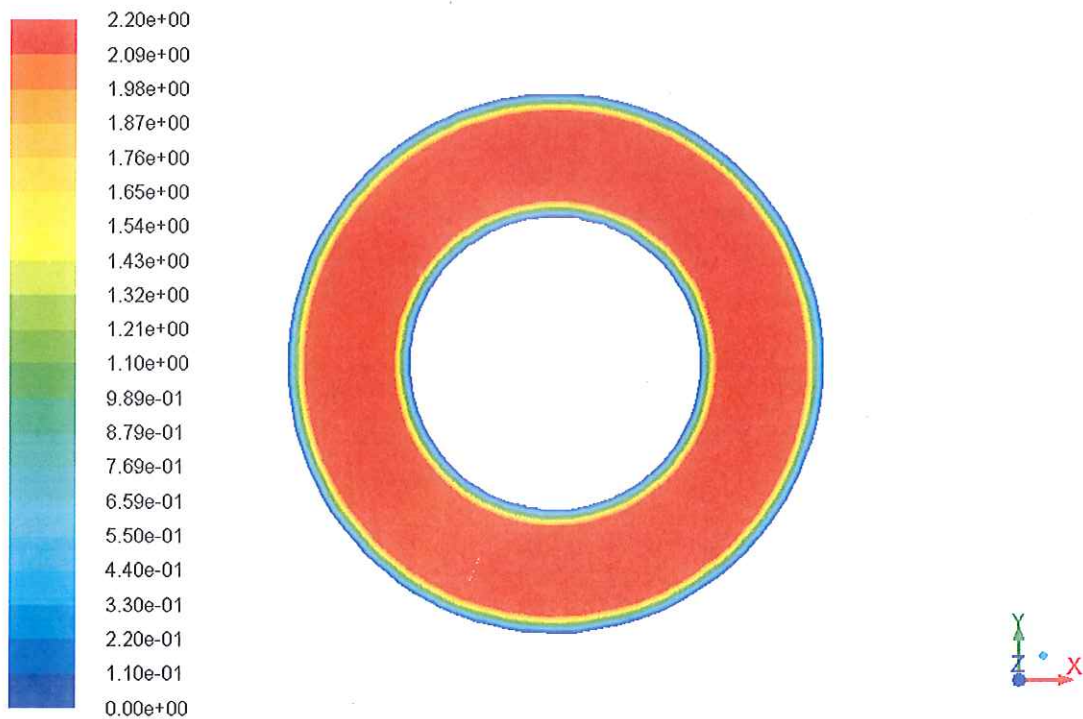


Fig 7

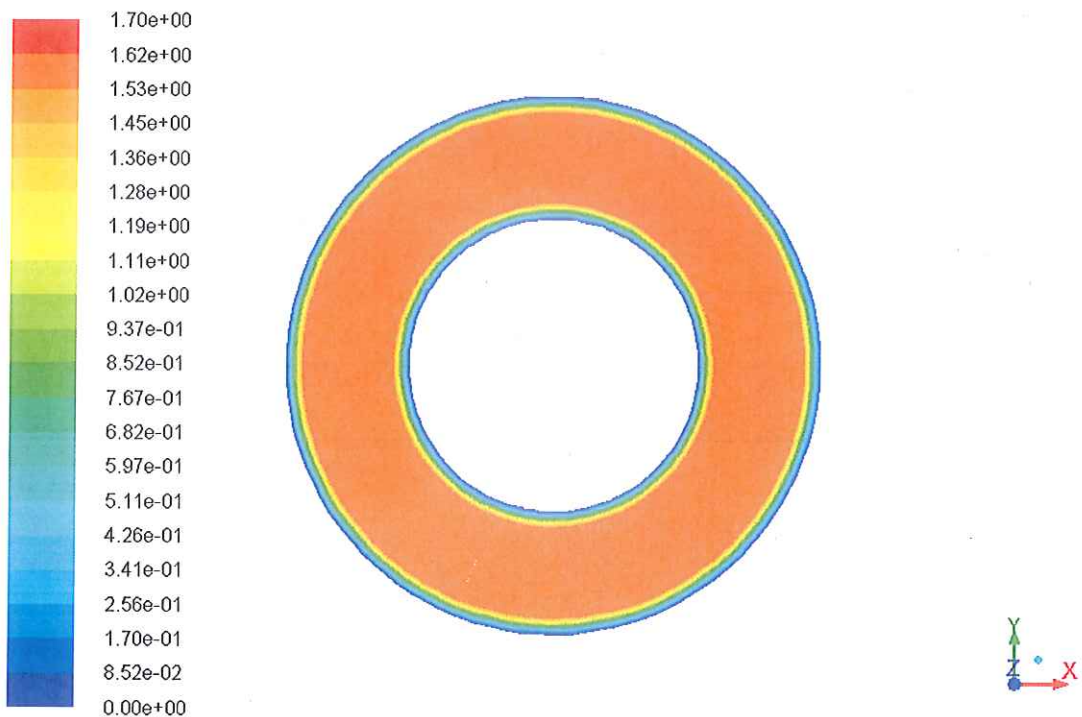


Contours of Velocity Magnitude (m/s)

(d)

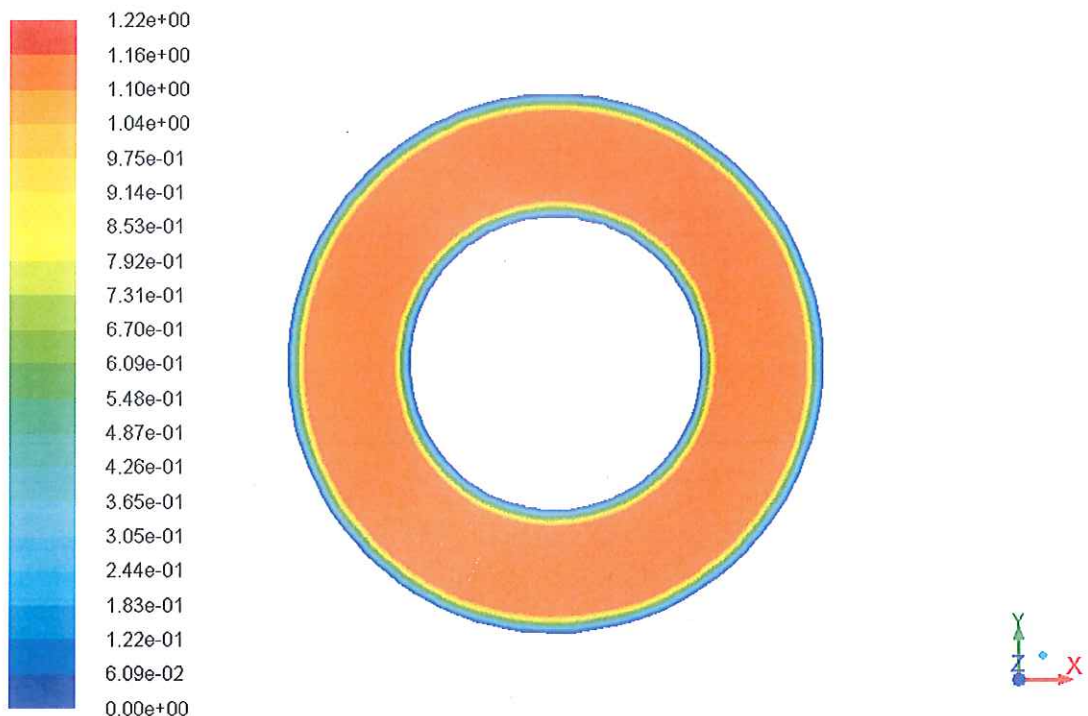
$V = 2. m/s$

Fig 6



Contours of Velocity Magnitude (m/s)

Fig 6 (c)
 $V_c \approx 1.5 \text{ m/s}$



Contours of Velocity Magnitude (m/s)

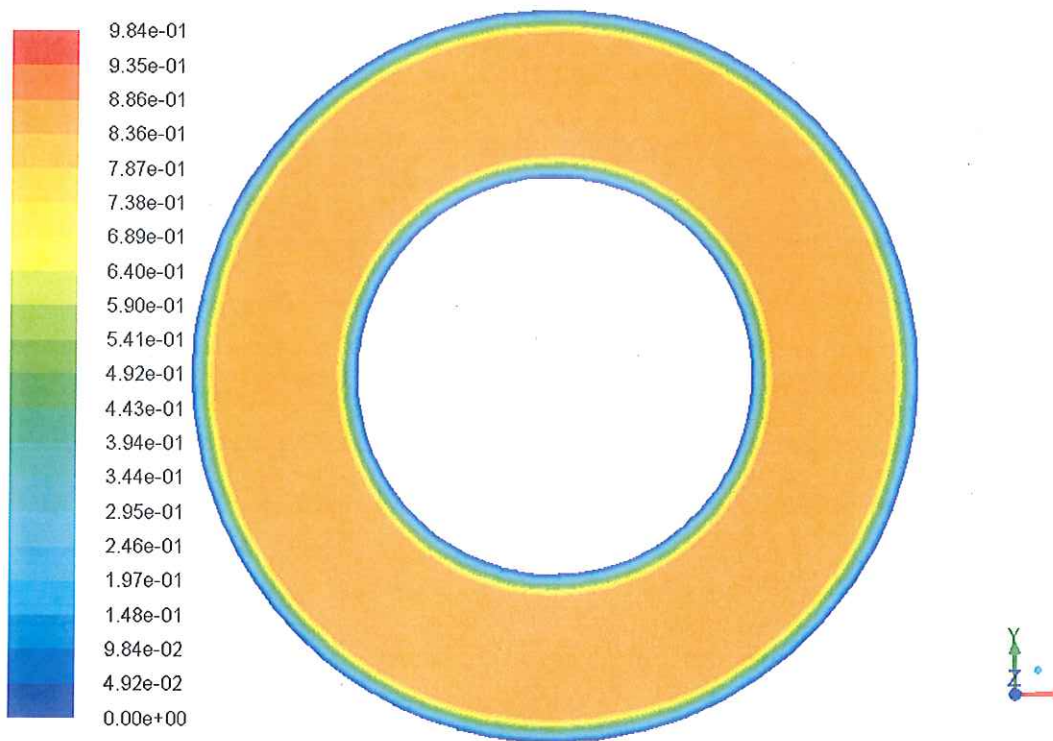
$$V = (\sim 1)_J$$

Fig 6

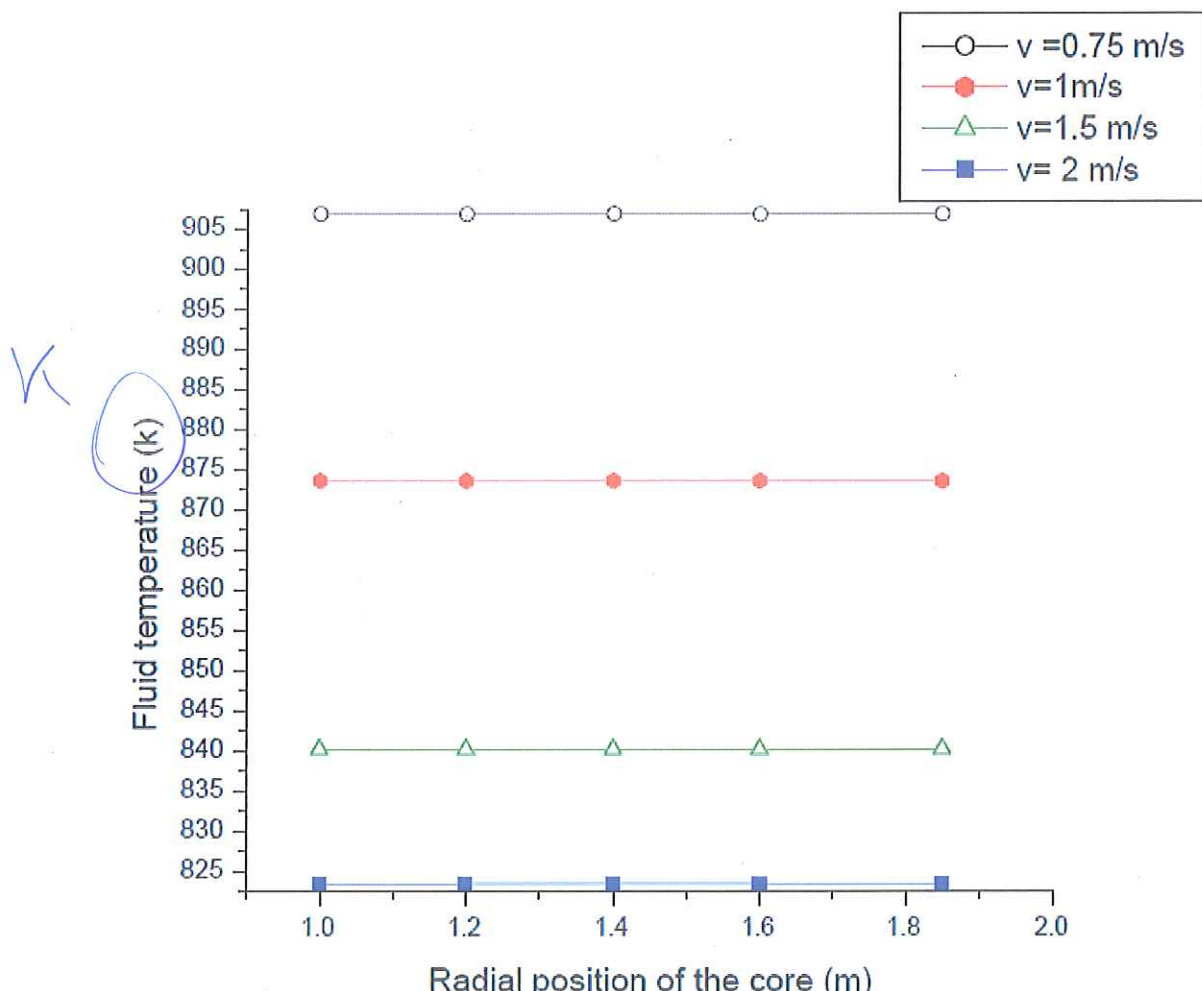
(b)

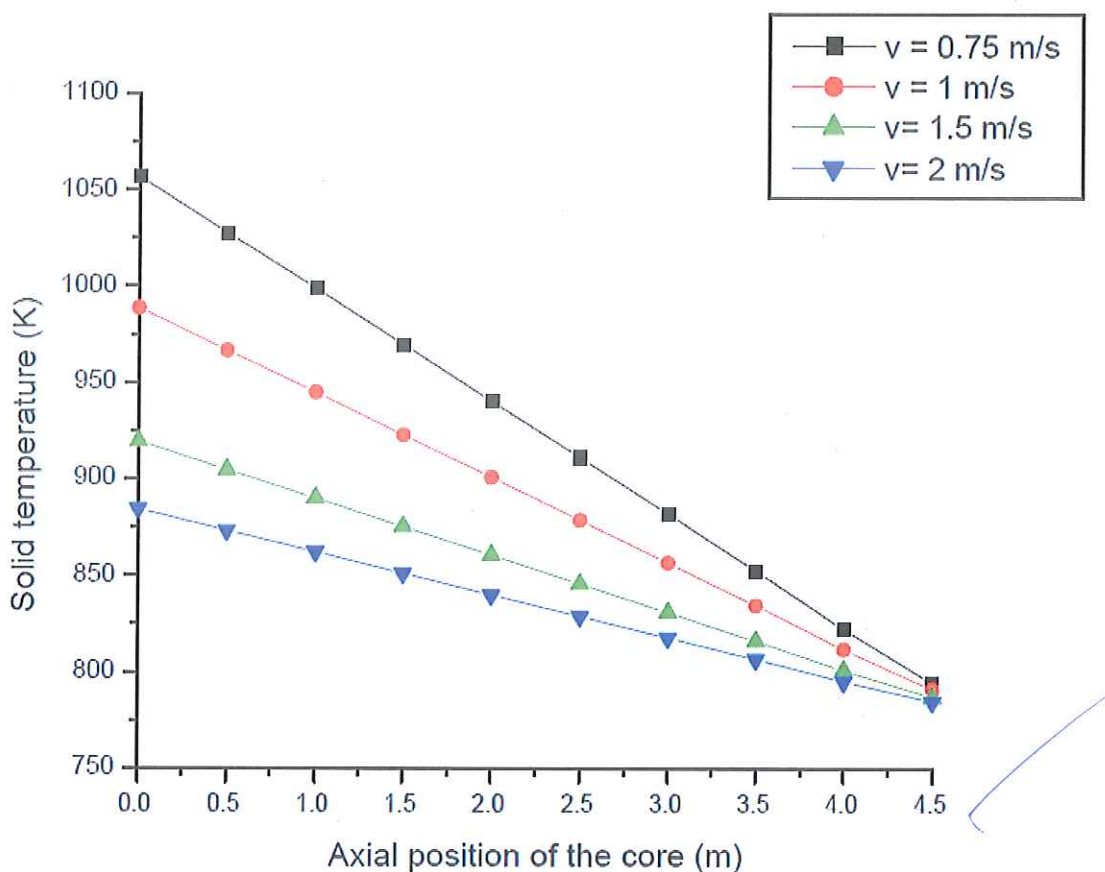
Figure

[Click here to download Figure fig6.doc](#)



$K_1 \sqrt{b}$ (a) $V = 0.25 \text{ m/s}$





(b)

Fig4
Unter Wohnung?

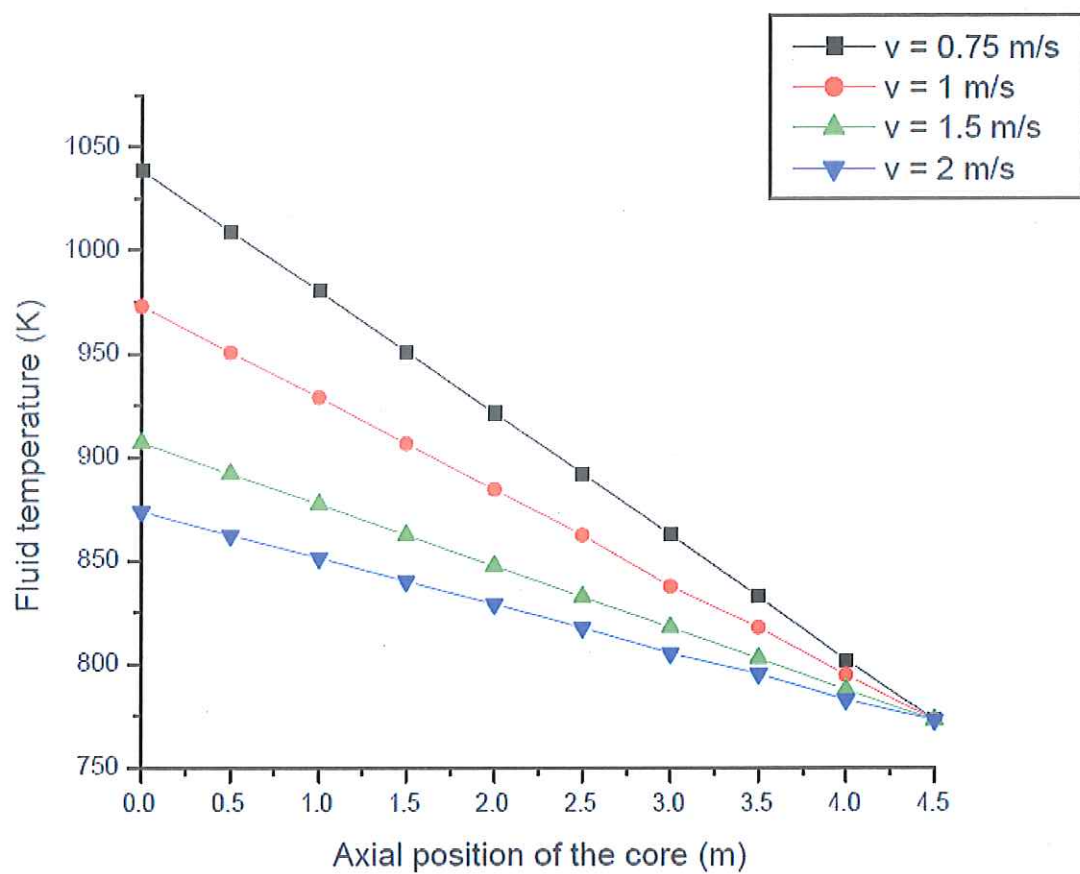


Fig 9

(a)

center up?

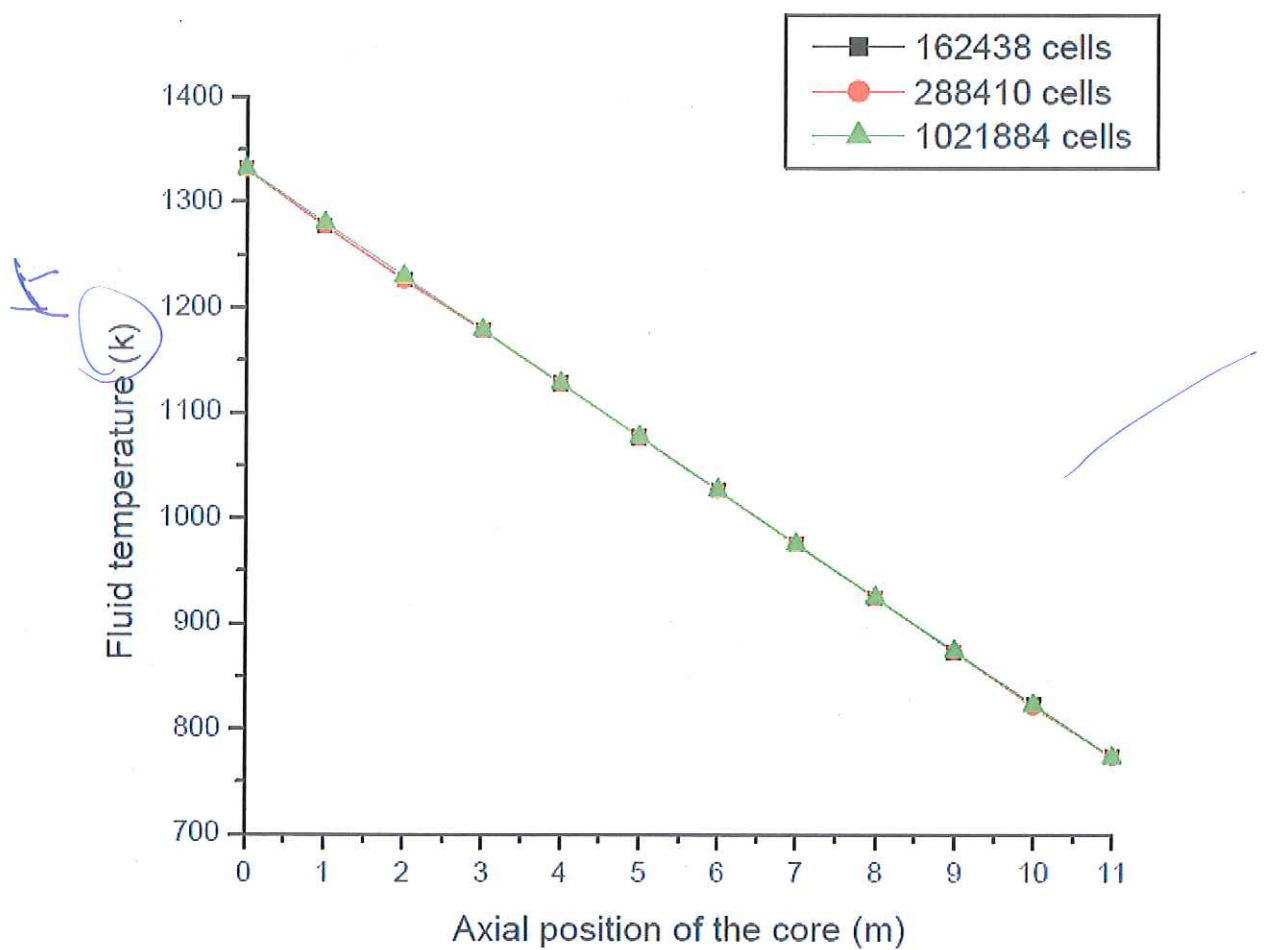


Fig3

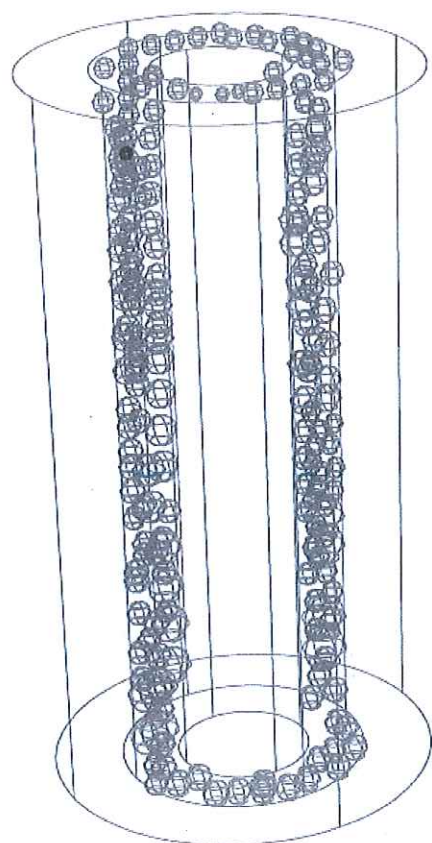


Fig2 *option 1*

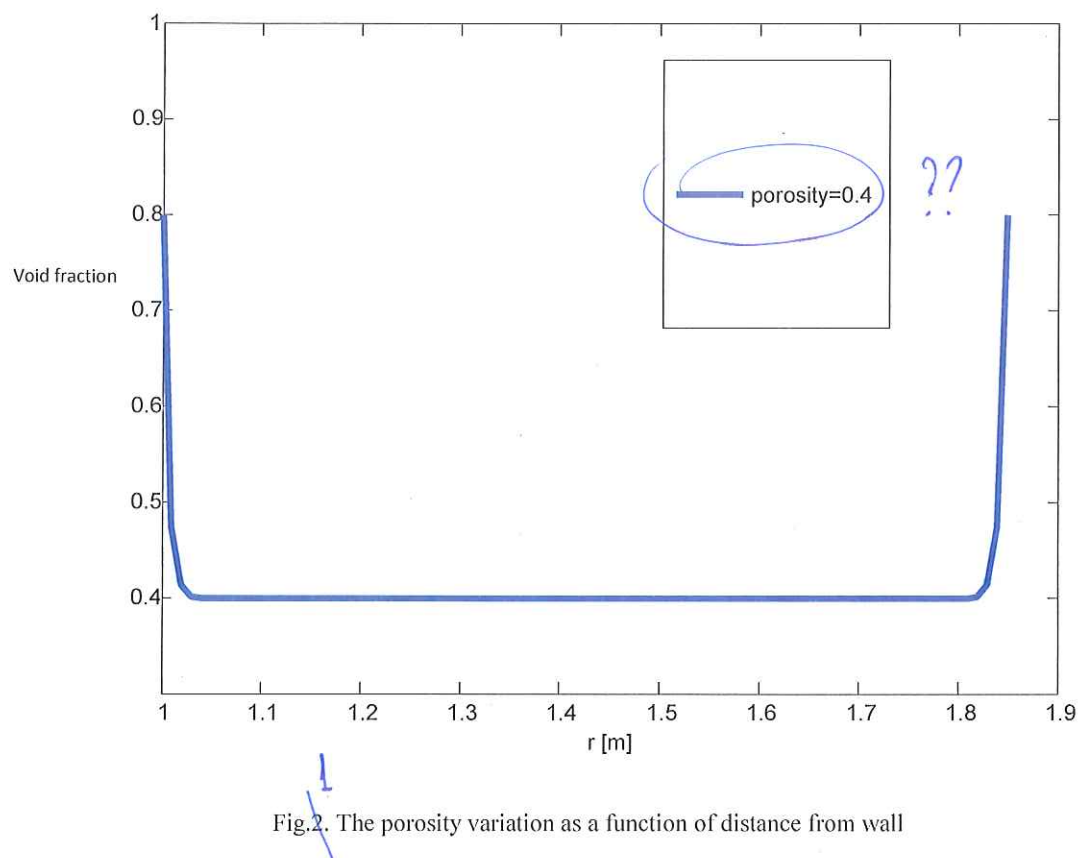


Table2

Computational boundary	Boundary conditions
Inlet	Mass flow-inlet
Outlet	Pressure-outlet
Bottom	Wall
Top	Wall
Surface of center reflector	Wall
Surface of side reflector	Wall